Research article

Assessment of Agricultural Land-use/ Land-cover Change in the Diamphwe River Basin using Sentinel-2 Imageries

KENFORD A. B. LUWEYA
Graduate School of Agro-Environmental Science, Tokyo University of Agriculture, Japan

KE ZHANG
Japan International Research Center of Agricultural Sciences, Japan

LAMECK FIWA
Lilongwe University of Agriculture and Natural Resources, Malawi

SARVESH MASKEY
Faculty of Regional Environmental Science, Tokyo University of Agriculture, Japan

AYAKO SEKIYAMA
Faculty of Regional Environmental Science, Tokyo University of Agriculture, Japan

HIROMU OKAZAWA*
Faculty of Regional Environmental Science, Tokyo University of Agriculture, Japan
Email: h1okazaw@nodai.ac.jp

Received 30 December 2024 Accepted 6 June 2025 (*Corresponding Author)

Abstract Land use and land cover (LU/LC) classification is an important aspect of research in various sectors of society. With technological advancements, LU/LC classification is a catalyst to achieve set goals, including the Malawi 2063 agenda. Diamphwe Basin, with over 90% farmers, is in central Malawi on vastly flat land, with a lot of potential in both commercial and subsistence agriculture production. Using the September 2017 and 2022 Sentinel-2 images, supervised classification and change detection were performed to track LU/LC changes using the maximum likelihood algorithm. The classes used for this classification were dense vegetation, wetland vegetation, agricultural land, settlement land, and bare land. The results showed that dense vegetation land increased by 10%, mostly converted from wetlands in forest reserves, and agricultural land decreased by 15.5%, of which a large proportion was converted to settlement land, thus increasing settlement land (urbanization) by 11.7%. The increased dense forest is expected to have a cooling effect and can increase baseflow to river discharge, whereas decreased agricultural land is expected to have a heating effect on the land mass. However, owing to the proximity to agricultural land, people in the basin experience more heating effects than cooling effects. Urbanization can create a ready market and can be leveraged to increase agricultural production through irrigation in the basin, as seen in the case of the Ganges River Basin. An increase in dense forest area could lead to an increase in river discharge owing to an increase in basin storage in the form of a baseflow increase. Since almost all human developments occur on land, LU/LC change detection is the key to policymakers and other stakeholders in achieving the three pillars of the Malawi 2063 agenda, thus agricultural development, industrialization, and urbanization by keeping abreast of the changes on the land.

Keywords Sentinel-2, LU/LC, change detection, classification method, agricultural land

INTRODUCTION

Land use and land cover (LU/LC) changes are important topics in various societal sectors. It refers to changes in the surface covering of the Earth and the conversion of land utilization by humans from

one purpose to another. Land/canopy cover is a significant indicator of crop development (Zhang et al. 2021). LU/LC classification is vital for urban planning, resource management, environmental monitoring, and agriculture (Topaloğlu et al., 2016). The Diamphwe Basin's long-term hydrologic trend analysis showed a decreasing trend in river discharge between 1975 and 2010 (Luweya et al., 2024); however, a recent half-decade hydrological trend indicates an increase in river discharge. Changes in LU/LC, such as the shift from perennial to seasonal vegetation (row-cropping/agricultural expansion), lead to increased discharge (water yield) owing to an increase in baseflow (Schilling et al., 2010). In small, forested watersheds, an increase in forest cover increases the base flow by promoting infiltration (sink function enhancement) and recharging-discharging processes that increase the yield at the outlet (Zhou et al., 2010; Ouyang et al., 2013; Uwimana et al., 2017).

Limited point-based weather data from traditional stations hamper climate-change research. RS provides a continuous, high-resolution view of the Earth's climate using satellite, aircraft, or drone sensors (Wang, 2023). Satellite RS technology data provide observations of essential climate variables (ECVs), such as LU/LC, independent of in situ measurements, thus enhancing our understanding of climate change from space by validating climate models and improving their future projections and impacts (Wang 2023; Zhao et al. 2023). LU/LC conversion impacts the climate through temperature changes; any change in agricultural land cover induces localized cooling, similar to reforestation, but converting dense forests to agriculture induces warming (Nayak and Mandal, 2019; Sleeter et al., 2018). Several LU/LC classification studies have been conducted in Malawi, ranging from monitoring forest resources in both urban and forest reserves, all of which used satellite sensors other than high spatial and temporal resolution, to Sentinel-2, which offers free access, a convenient option for developing countries such as Malawi. Most of the previous RS research could not target agricultural watersheds such as the Diamphwe Basin, where climate change issues can be leveraged through LU/LC changes, especially in developing countries where point weather data are scarce.

OBJECTIVE

Hydrologic trends for river discharge indicate an increasing trend in the last seven years, despite long-term decreasing trends over the past 3.5 decades. To understand the cause of the recent increasing trend of river discharge, this study aimed to detect six years of LU/LC changes in the Diamphwe agricultural watershed using Sentinel-2 imagery.

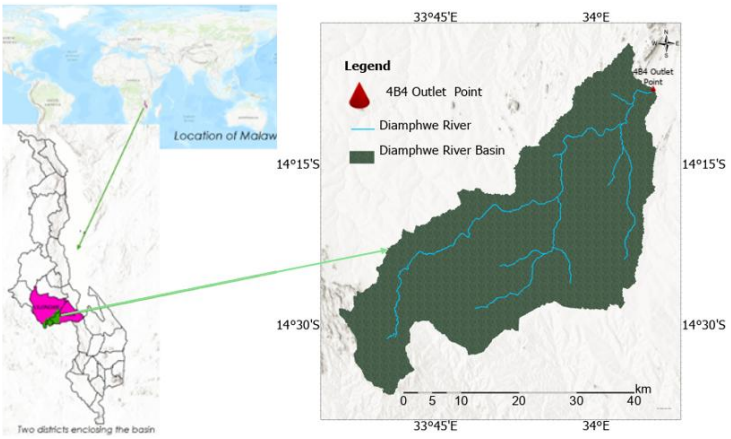

Fig. 1 Location of Diamphwe River basin

ETHODOLOGY

Study Site

The Diamphwe River Basin (Fig. 1) has vast wetlands (Dambos) along the perennial river with high irrigation potential that stakeholders have not yet fully utilized. It covers the Lilongwe and Dedza districts within the central region plains between 1,200 and 1,400 m above sea level. The basin has a warm tropical climate with temperatures ranging from 3.5°C to 39°C; generally, it has a rainy season (November to April) and a dry season (May to October) (Malawi Government, 2016). Similar to the rest of the country, rainfed agriculture is the main occupation of the basin, with over 90% of the farmers being small-scale (Malawi Government, 2019). The basin is located between 33.57°E and 34.13°E and 13.96°S and 14.72°S, enclosing an area of 1420.2 km^2. The Dzalanyama Forest Reserve partly occupies the basin within the river catchment area bordering Mozambique.

Data Collection and Pre-Processing

Earth observation (EO) Sentinel-2 and 12 band-based raw data images were downloaded from the Sentinel Hub website to assess LU/LC changes. The details of downloaded data are as follows.

Table 1 Sentinel-2 data details

Parameter	Details
Data source/format	Sentinel 2 EO browser/ TIFF (32-bit float)
Resolution/coordinate system	High (2500 x 1449px)/ WGS (EPSG 4326)
Resolution	Lat: 0.0006871 deg/px (2.5sec/px); Long : 0.0007086 deg/px (2.6sec/px)
Cloud cover	Atmospherically corrected (cloud cover < 5%)
Download/ recorded date	6th August 2024/ 1st September 2017 and 23rd September 2022

After the data were downloaded, composite band combinations were prepared in ArcGIS Pro to produce RGB composites (true color →B04, B03, and B02, or false color → B05, B04, and B03). For clear vegetation identification, a Normalized Difference Vegetation Index (NDVI) composite raster was prepared (B04→ electromagnetic spectrum (EMS) portion that absorbs red energy and resampled to 10 m resolution B08→EMS portion that reflects NIR energy) for use with (RGB=Red, Green, Blue) composites. NDVI was computed (Rouse et al., 1973) as shown in Eq. (1).

$$\mathrm{NDVI} = \frac{\mathrm{NIR} - \mathrm{Red}}{\mathrm{NIR} + \mathrm{Red}} \quad (1)$$

where NIR is the near-infrared energy reflected and Red is the energy absorbed within the EMS.

Image Classification and Method

Supervised image classification was used in this study, where the image analyst guided the pixel categorization process by providing numerical descriptors for different LU/LC types in the scene to a computer algorithm (Sivakumar et al., 2003). Using representative sample sites of known LU/LC types (training samples), a numerical interpretation key was created to outline the spectral attributes for each feature. In ArcGIS Pro, each pixel in the dataset was compared numerically to each category in the interpretation key and labelled with the name of the category it most closely resembled (Sivakumar, 2012). Table 2 describes the five classes utilized since the data were collected in September, the dry season.

Table 2 Class descriptions and codes

Code	Class	Description
1	Dense vegetation	Areas with thick vegetation, especially in natural forest reserves
2	Vegetation/wetlands	Areas with trees, shrubs and bushes, especially in dambos/forests
3	Agriculture/cultivated land	Land used for cultivation of crops, especially rainfed crops
4	Settlement/build-up land	Residential areas and trading centers with some buildings
5	Bare land	Areas with no vegetation and not used for cultivation, also in forest

GIS has three main methods for classifying satellite images: (1) maximum likelihood (ML), (2) Geoprocessing Tool-classified raster (GPT-CR), and (3) image classification wizard (ICW) with

three sub-methods: SVM, RT, and KNN. The GPT-CR classification method was used in this study after proving to be a better classifier for Sentinel-2 images than the other methods.

Accuracy Assessment and Change Detection

An accuracy assessment compares a classified image to a reference image, such as an aerial photograph or ground truth data, by matching pixels for pixels in scale, detail, categories, and projection (Parece et al., 2019). An accuracy assessment point raster was created and linked to Google Earth using a Keyhole Markup Language (KML) file. Google Earth uses more recent images as ground truth for study regions. Pixel mismatches in the RS are recorded as errors in an error matrix that compares the class code assigned during classification with the actual class from an aerial photo. The two key coefficients from the error matrix are (i) Cohen's kappa, which assesses the classification performance against random assignment, and (ii) overall accuracy, which indicates the ratio of matching points between the classified and reference images (Parece et al., 2019). Change detection in RS involves comparing multiple pairs of raster datasets from the same area at different times to identify the type, magnitude, timing, and location of changes due to environmental or climatic trends. Hence, the output is the difference between the raster in pixel changes (Parece et al., 2019). In this study, two classified rasters, 2017 and 2022 Sentinel-2, classified raster for the Diamphwe Basin, were used. Raster was first converted from the crf format to TIFF and then to a polygon raster. The dissolved polygon raster generated a 'from → to Table' through a pixel-by-pixel comparison to allow the assessment of the nature and magnitude of change, as shown in area and percentages in Table 6.

RESULTS AND DISCUSSION

The MK/Pettitt test for the 2010-2023 rainfall trend decreased (not significant) and river discharge trend increased 2018 as a transition year (at a 0.10 significance level) between a set of years with lower and a set of years with higher river discharge (Fig. 2, left); hence, diverged rainfall-river discharge trends. For the years with higher river discharges, 2016-2023, an increasing trend (MK trend analysis) was obtained (at a significance level of 0.01) (Fig. 2, right). However, rainfall showed no trend change in the two R-analyses, that is, the MK and Pettitt tests. To assess the linkages between increasing river discharge and basin characteristics, RS and ArcGIS methods and LU/LC changes were analyzed. Hence, LU/LC change detection was performed using Sentinel-2 images from 2017 and 2022. The classified rasters were assessed for accuracy, and the results are summarized in the accuracy assessment Tables 3 and 4.

The overall accuracy and kappa coefficients for 2022 were 77% and 69%, respectively, whereas those for 2017 were 81% and 74%, respectively. A higher kappa coefficient indicates a better classification process than the random assignment of values. However, a higher overall accuracy indicates a good match between the classified and reference images, such as those from Google Earth.

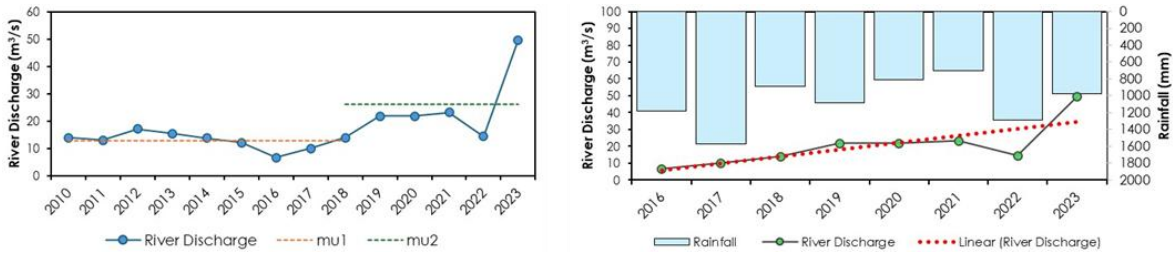

Fig. 2 Pettitt test for 2010-2023 (left) and MK trend for 2016-2023 (right)

Change Detection

Figure 3 shows the classified raster for 2017 and 2022, and Tables 5 and 6 show the changes detected in the area (km^2) and percentage ratios over the six years, respectively. Dense vegetation increased by 10.03%, from 136.64 km^2 in 2017 to 150 km^2 in 2022. Notably, 12.6% of wetland vegetation (54.01 km2) was converted to dense vegetation between 2017 and 2022, representing 3.82% of the entire basin area (Table 5).

Table 3 Confusion matrix assessment for 2017

	Dense veg.	Wetlands	Agriculture	Settlement	Bare land	Total	P-accuracy	Kappa
Dense Veg.	11	0	0	0	0	11	1.00	0
Wetlands	0	32	1	0	0	33	0.97	0
Agriculture	3	3	38	1	0	45	0.84	0
Settlement	5	0	5	10	0	20	0.50	0
Bare land	0	1	4	0	5	10	0.50	0
Total	19	36	48	11	5	119	0.00	0
P-accuracy	0.58	0.89	0.79	0.91	1.00	0.00	0.81	0
Kappa	0	0	0	0	0	0	0	0.74

Table 4 Confusion matrix assessment for 2022

	Dense veg.	Wetlands	Agriculture	Settlement	Bare land	Total	P-accuracy	Kappa
Dense Veg.	8	3	0	0	0	11	0.73	0
Wetlands	0	32	1	0	0	33	0.97	0
Agriculture	0	3	32	0	0	35	0.91	0
Settlement	0	1	9	11	0	21	0.52	0
Bare land	0	8	0	0	2	10	0.20	0
Total	8	47	42	11	2	110	0.00	0
P-accuracy	1	0.68	0.76	1.00	1.00	0.00	0.77	0
Kappa	0	0	0	0	0	0	0.00	0.69

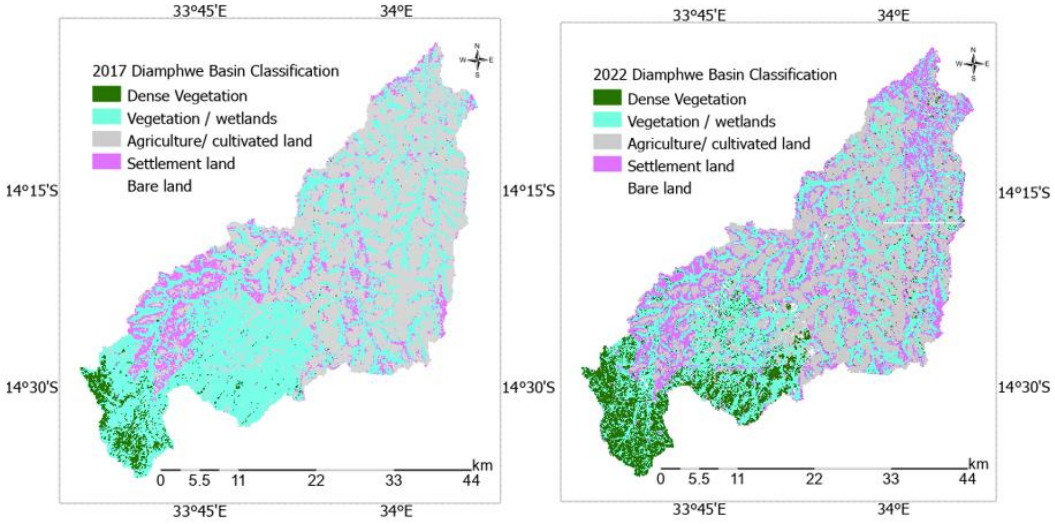

Fig. 3 2017 and 2022 classified raster for Diamphwe basin

Wetland (Dambo) vegetation increased by 11.14% from the initial area of 428.72 km^2 in 2017, specifically in the protected areas of the Dzalanyama and Chongoni forest reserves. An increase in dense forests leads to general cooling conditions (Sleeter et al., 2018). The increase in dense vegetation could have resulted from the intensified security of the Malawi Defense Forces (MDF) over the last decade, especially in areas far from people where security is tight.

Some areas with dense vegetation were possibly reclaimed land encroached upon from the late 1990s to the early 2000s. Agricultural land decreased by 15.49% (91.33 km^2). Notably, 15.49% (91.31 km^2) (Table 5) of agricultural land was converted to settlements, representing 6.45% of the basin area. The increase in dense vegetation in the interiors of the two forest reserves, Chongoni and

Dzalanyama, has less impact on land cooling because dense vegetation is far from where people live. People are more affected by warming owing to the decreased agricultural land.

Increased perennial dense vegetation can contribute to the river's baseflow due to the promotion of infiltration-recharge-discharge processes that increase basin storage, consequently redistributing water from the rainy season to the dry season. The conversion of agricultural land to settlement land can accelerate river sedimentation due to increased surface runoff (Schilling et al. 2010; Uwimana et al. 2017; Zhou et al. 2010).

Table 5 Detailed actual 2017-2022 changes detected in each class

Code	Class name	Initial area (km^2)	Initial % Δ	2022-2017 area Δ (km^2)	Basin% area Δ
1	Dense vegetation to wetlands	136.64	34.05	46.52	3.29
2	Dense vegetation to Agriculture land	136.64	7.99	10.92	0.77
3	Dense vegetation to Settlement land	136.64	2.57	3.51	0.25
4	Dense vegetation to Bare land	136.64	1.15	1.57	0.11
5	Wetlands to Dense vegetation	428.72	12.60	54.01	3.82
6	Wetlands to Agriculture land	428.72	6.61	28.35	2.00
7	Wetlands to Settlement land	428.72	7.42	31.80	2.25
8	Wetlands to Bare land	428.72	0.57	2.43	0.17
9	Agriculture land to Dense vegetation	589.64	3.10	18.25	1.29
10	Agriculture land to Wetlands	589.64	12.05	71.03	5.02
11	Agriculture land to Settlement land	589.64	15.49	91.31	6.45
12	Agriculture land to Bare land	589.64	0.44	2.61	0.18
13	Settlement land to Dense vegetation	256.96	1.76	4.53	0.32
14	Settlement land to Wetlands	256.96	15.91	40.88	2.89
15	Settlement land to Agriculture land	256.96	21.27	54.67	3.86
16	Settlement land to Bare land	256.96	0.42	1.09	0.08
17	Bare land to Dense vegetation	7.25	1.76	0.13	0.01
18	Bare land to Wetlands	7.25	18.67	1.35	0.10
19	Bare land to Agriculture land	7.25	6.89	0.50	0.04
20	Bare land to Settlement land	7.25	76.48	5.55	0.39
21	No change			944.79	66.73
	Total Area			1415.82	100.00

Table 6 Area contribution per class for 2017 and 2022 classified raster

Class name/code	2017		2022		Area Δ	Percent Δ
	Area (km^2)	Percent	Area (km^2)	Percent		
Dense vegetation	136.64	9.63	150.35	10.59	13.71	10.03
Vegetation/ wetlands	428.72	30.21	476.47	33.57	47.75	11.14
Agriculture/ cultivated land	589.64	41.54	498.31	35.11	-91.33	-15.49
Settlement land	256.96	18.10	286.91	20.21	29.95	11.66
Bare land	7.25	0.51	7.35	0.52	0.09	1.31

CONCLUSION

RS and GIS are vital for classifying and detecting changes in satellite imagery. Using Sentinel-2, five classes were classified in the Diamphwe Basin: dense vegetation, wetland vegetation, agricultural land, settlement land, and bare land. The GPT-CR method was used for supervised classification during the 6-year study period from 2017 to 2022. A total of 66.7% of the basin land was not exposed to any changes in LU/LC. Agricultural land experienced a decrease of 15.5%, of which a large proportion was converted to settlement land, resulting in an increase in settlement land (urbanization) of 11.7%. Within the forest region, dense vegetation experienced an increase in area of 10.0%, largely converted from wetland vegetation. Cooling conditions are expected from an increase in dense vegetation in the forest; however, decreasing agricultural land has a heating effect on the basin. People in the basin experience a heating effect more than a cooling effect because they are closer to agricultural land than to dense vegetation land. Government land reclamation efforts through tight MDF security could have contributed to the increased density of vegetation in the forest. Increased

dense perennial vegetation can contribute to river baseflow, which can increase the river discharge. The decrease in farmland is a worrisome situation for the basin, as over 90% of the inhabitants are farmers. Increased urbanization can mean an expansion of the market for farm goods that can be leveraged by venturing into modern irrigation to increase production. Increased settlement land and decreased wetland vegetation accelerate sedimentation in rivers because of increased surface runoff. This research recommends a combined field and RS study of river ecotone (Dambos) analysis and watershed modelling to quantify the water yield and sediments. LU/LC change detection is key to policy-makers and stakeholders achieving the three pillars of the Malawi 2063 agenda by keeping abreast of land changes.

ACKNOWLEDGEMENTS

We acknowledge the financial and technical support provided by the Hydrostructural Engineering Laboratory and the Tokyo University of Agriculture. We also thank the World Bank through the Domasi College of Education for financial support through a scholarship awarded to the first author.

REFERENCES

Luweya, K., Fiwa, L., Zhang, K., Maskey, S., Gono, H. and Okazawa, H. 2024. Long-term hydrologic trend analysis of the Diamphwe River basin in Central Malawi. International Journal of Environmental and Rural Development [accepted and in press].

Malawi Government. 2016. Diamphwe multipurpose dam & associated structures ESIA and RAP. Volume 1 Main Report Environmental & Social Impact Assessment Draft Report SFG1799 V1, Retrieved from URL www.smec.com

Malawi Government. 2019. Integrated Household Survey: NSO, Retrieved from URL http://www.nsomalawi.mw/images/IHPS_2010-2019_Final_REPORT.pdf

Nayak, S. and Mandal, M. 2019. Impact of land use and land cover changes on temperature trends over India. Land Use Policy, 89, 104238, Retrieved from DOI https://doi.org/10.1016/j.landusepol.2019.104238

Ouyang, Y., Leininger, T.D. and Moran, M. 2013. Impacts of reforestation upon sediment load and water outflow in the lower Yazoo River watershed, Mississippi. Ecological Engineering, 61, 394-406, Retrieved from https://doi.org/10.1016/j.ecoleng.2013.09.057

Parece, T.E., McGee, J.A. and Campbell, J.B. 2019. Remote sensing with ArcGIS Pro. America view consortium, Retrieved from URL https://landsat.visibleearth.nasa.gov

Rouse, J.W., Haas, R.H., Schell, J.A., Deering, D.W. and Harlan, J.C. 1973. monitoring the vernal advancement 1 and retrogradation (green wave effect) of natural vegetation. Retrieved from https://ntrs.nasa.gov/api/ citations/19750020419/downloads/19750020419.pdf

Schilling, K.E., Chan, K.S., Liu, H. and Zhang, Y.K. 2010. Quantifying the effect of land use land cover change on increasing discharge in the upper Mississippi River. Journal of Hydrology, 387 (3-4), 343-345, Retrieved from https://doi.org/10.1016/j.jhydrol.2010.04.019

Sivakumar, M.V.K., Roy, P.S., Harmsen, K. and Saha, S.K. 2003. Satellite remote sensing and GIS applications in agricultural meteorology. World Meteorological Organization, Geneva, Switzerland, Retrieved from URL https://www.unisdr.org/files/1682_9970.pdf

Sivakumar, V. 2012. Remote sensing and image interpretation-spectral signature. Chapter, 41, 54, SN 978-81-266-5966-1, Retrieved from https://www.researchgate.net/publication/250614472

Sleeter, B., Loveland, T.R., Domke, G.M., Herold, N., Wickham, J. and Wood, N.J. 2018. Chapter 5 : Land cover and land use change. Impacts, Risks, and Adaptation in the United States: The Fourth National Climate Assessment, Volume II, Retrieved from https://doi.org/10.7930/NCA4.2018.CH5

Topaloğlu, R.H., Sertel, E. and Musaoğlu, N. 2016. Assessment of classification accuracies of Sentinel-2 and Landsat-8 data for land cover/use mapping. ISPRS International Journal of Geo-Information Archives, 41, 1055-1059, Retrieved from https://doi.org/10.5194/isprsarchives-XLI-B8-1055-2016

Uwimana, A., van Dam, A., Gettel, G., Bigirimana, B. and Irvine, K. 2017. Effects of river discharge and LULC on water quality dynamics in Migina catchment, Rwanda. Environmental Management, 60 (3), 496-512. Retrieved from DOI https://doi.org/10.1007/s00267-017-0891-7

Wang, X. 2023. Remote sensing applications to climate change. Remote sensing, 15 (3), 747, Retrieved from https://doi.org/10.3390/rs15030747

Zhang, K., Okazawa, H., Yamazaki, Y., Hayashi, K. and Tsuji, O. 2021. Relationship between NDVI and

canopy cover sensed by small UAV under different ground resolution. International Journal of Environmental and Rural Development, 12 (2), 122-128, https://doi.org/10.32115/ijerd.12.2_122

Zhao, S., Liu, M., Tao, M., Zhou, W., Lu, X., Xiong, Y., Li, F. and Wang, Q. 2023. The role of satellite remote sensing in mitigating and adapting to global climate change. Science of The Total Environment, 904, 166820, Retrieved from DOI https://doi.org/10.1016/j.scitotenv.2023.166820

Zhou, G., Wei, X., Luo, Y., Zhang, M., Li, Y., Qiao, Y., Liu, H. and Wang, C. 2010. Forest recovery and river discharge at the regional scale of Guangdong province, China. Water Resources Research, 46 (9). Retrieved from DOI https://doi.org/10.1029/2009WR008829